Thermochimica Acta, 74 (1984) 255–272
Elsevier Science Publishers B.V., Amsterdam – Printed in The Netherlands

KINETICS OF THE DECOMPOSITION OF HYDRATED OXALATES OF CALCIUM AND MAGNESIUM IN AIR

AHMED M.M. GADALLA

Chemical Engineering Department, Texas A and M University, College Station, TX 77843 (U.S.A.)

(Received 26 September 1983)

ABSTRACT

Combined thermal analysis was used to establish the dissociation steps for the hydrated oxalates of calcium and magnesium. While dehydration of calcium oxalate monohydrate is governed by three-dimensional phase boundary movement, dehydration of magnesium oxalate is governed by Avrami–Erofeev nuclei growth. Both dehydration reactions demonstrated that the activation energy and the pre-exponential factor vary with temperature over wide ranges. Accordingly, the methods of Reich and Kissinger (based on the maximum rate temperature) or Carroll and Manche are not suitable. Moreover they could not distinguish between the overlapping reactions or mechanisms. They can be only used as a guide in differentiating between the possible mechanisms obtained using the methods of Coats and Redfern or Šatava and Škvàra. The latter method is recommended since it gives a smaller number of possible operating mechanisms. When possible mechanisms have close activation energies both techniques are needed.

Both anhydrous oxalates dissociated to the carbonates according to the Avrami–Erofeev nuclei growth, A_2. For the magnesium salt, at low heating rates, this step was accompanied by dissociation of $MgCO_3$ to MgO. Both carbonates dissociate according to a three-dimensional phase boundary migration mechanism.

NOTATION

A = frequency factor (pre-exponential factor for Arrhenius equation)
d = interplanar distances in crystals
E = activation energy (kcal mol^{-1})
K = constant rate
m = mass at the beginning of step
m_v = mass at the end of step
m_t = mass at temperature T
n = apparent reaction rate
$p(x) = e^{-x}/x - \int_x^\infty (e^{-x}/x)dx = e^{-x}(1!/x^2 - 2!/x^3)$ (see ref. 19)
R = universal gas constant
t = time

0040-6031/84/$03.00

T = absolute temperature
x = $-E/RT$
α = decomposed fraction = $(m_0 - m_t)/(m_0 - m_v)$
β = heating rate dT/dt

INTRODUCTION

While extensive work has been carried out on the dissociation kinetics of calcium oxalate monohydrate and on the calcination of calcium carbonate, nothing was reported on the dissociation of hydrated magnesium carbonate. Since most of the previous authors treated heterogeneous reactions as homogeneously, a theoretical section is added to review methods for analyzing thermogravimetric curves.

In this paper, various methods were applied to the established steps for the dissociation of hydrated calcium oxalate and were compared with previous findings. Similar procedures were adopted to determine the mechanisms and the kinetic parameters for the dissociation of hydrated magnesium oxalate. In view of the difficulties encountered, the above methods are assessed and the best procedure, to treat similar results, is recommended.

THEORY

Due to the limited information on heterogeneous reactions most research workers adopted equations established for homogeneous reactions and considered the reaction rate to be proportional to the nth power of the unreacted material

$$d\alpha/dt = k(1-\alpha)^n \tag{1}$$

In heterogeneous reactions, there is a reaction interface between the reacting phases and after formation of stable nuclei and their growth above the critical size, some of (or all) the following steps take place: mass transfer to the interface; reaction at the boundary; and mass transfer of the products away from the interface or grain boundary movement. The reaction at the phase boundary liberates heat or absorbs heat, changing its temperature, and accordingly heat transfer to or from the boundary may limit the rate of the process. The slowest of these steps will be the rate-determining step.

Astonishingly, the results obtained for heterogeneous reactions fit well to the reaction order equation in spite of the fact that eqn. (1) is correct for homogeneous reactions and that the physical meaning of the reaction order (n) no longer holds. The equations developed can have theoretical significance only in those cases where the value of n is 0, 1/2, 2/3 or 1 [1]. These values correspond to the following rate-controlling steps:

$n = 0$, one-dimensional movement of phase boundary or zero reaction order;

$n = 1/2$, two-dimensional movement of phase boundary (contracting cylinder); and

$n = 2/3$, three-dimensional movement of phase boundary (contracting sphere).

The rate constant k was considered to be related to temperature by the Arrhenius equation

$$k = Ae^{-E/RT} \tag{2}$$

This equation is only correct for activated processes such as diffusion processes but cannot be used for non-activated processes such as heat transfer. The reacting particles are not free and accordingly "A", which is taken in gases and liquids as the frequency factor and is proportional to the number of successful collisions of the reacting molecules, can be taken here only as a pre-exponential constant.

The rate equation can be written for isothermal processes in the general form

$$d\alpha/dt = kf(\alpha) \tag{3}$$

For the constant heating rate "β" for activated processes, eqns. (2) and (3) can be combined to give

$$\beta d\alpha/dT = Af(\alpha)\, e^{-E/RT} \tag{4}$$

$$\ln[\beta d\alpha/dT] = \ln[A.f(\alpha)] - E/RT \tag{5}$$

If $f(\alpha)$ is unknown, Carroll and Manche [2] showed that the activation energy can be calculated by plotting $\ln(\beta d\alpha/dT)$ vs. $1/T$ at a fixed value of α obtained from a series of TG curves at different heating rates.

The reaction mechanism may be determined by comparing the experimental data for a single TG curve with the various kinetic equations (Table 1) using eqn. (4).

The above methods depend on determining the first derivative and are thus known as differential methods. Integral methods can be deduced by rearranging eqn. (4)

$$d\alpha/f(\alpha) = [A/\beta]\, \exp(-E/RT)dT \tag{6}$$

Integrating eqn. (6) and replacing $\int d\alpha/f(\alpha)$ by the function $g(\alpha)$, which is shown for various mechanisms in Table 1, the equation for the TG curve can be obtained

$$g(\alpha) = [A/\beta] \cdot \int \exp(-E/RT)dT \tag{7}$$

To find the values of $g(\alpha)$ earlier workers [3–5] expressed the exponential part (roughly) in terms of the maximum reaction-rate temperature (T_m). These methods give accurate results only if the reactions proceed over

TABLE 1

Kinetics of heterogeneous solid-state reactions

Rate-determining mechanism	Symbol	$f(\alpha)$	$g(\alpha)=\int_0^\alpha d\alpha/f(\alpha)$
Nucleation and nuclei growth			
(1) Random nucleation: with one nucleus in each individual particle (Mampel unimolecular law)	F_1	$1-\alpha$	$-\ln(1-\alpha)$
(2) Avrami–Erofeev nuclei growth:			
Two-dimensional growth	A_2	$2(1-\alpha)[-\ln(1-\alpha)]^{1/2}$	$-[\ln(1-\alpha)]^{1/2}$
Three-dimensional growth	A_3	$3(1-\alpha)[-\ln(1-\alpha)]^{2/3}$	$-[\ln(1-\alpha)]^{1/3}$
Prout–Thompkins branching nuclei	A_1	$\alpha(1-\alpha)$	$\ln[\alpha/(1-\alpha)]$
Diffusion			
Parabolic law (one-dimensional transport process)	D_1	α^{-1}	$\alpha^2/2$
Valensi two-dimensional diffusion (cylinder with no volume change)	D_2	$[-\ln(1-\alpha)]^{-1}$	$(1-\alpha)\ln(1-\alpha)+\alpha$
Three-dimensional diffusion [spherical symmetry (Jander mechanism)]	D_3	$(1-\alpha)^{1/3}[(1-\alpha)^{-1/3}-1]^{-1}$	$1.5[1-(1-\alpha)^{1/3}]^2$
Three-dimensional diffusion (Brounshtein–Ginstling mechanism)	D_4	$[(1-\alpha)^{-1/3}-1]^{-1}$	$1.5[1-2\alpha/3-(1-\alpha)^{2/3}]$
Phase boundary movement			
One-dimensional (zero order)	R_1	constant	α
Two-dimensional (cylindrical symmetry)	R_2	$(1-\alpha)^{1/2}$	$2[1-(1-\alpha)^{1/2}]$
Three-dimensional (spherical symmetry)	R_3	$(1-\alpha)^{2/3}$	$3[1-(1-\alpha)^{1/3}]$
Power law		$(1-\alpha)^n$	$[1-(1-\alpha)^{1-n}]/(1-n)$

narrow temperature ranges (0.9 T_m–1.1 T_m). The equations proposed by Reich [5] can be used for results obtained at two different heating rates.

$$E = \frac{2.303R \log \frac{\beta_2}{\beta_1}\left[\frac{T_1}{T_2}\right]^2}{\frac{1}{T_1} - \frac{1}{T_2}} \tag{8}$$

Accurate results can also be obtained using the Coats–Redfern approximation [6]. Although their initial equations were derived assuming a power-law mechanism, they could be modified and generalized to suit heterogeneous reactions

$$\log \frac{g(\alpha)}{T^2} = \log \frac{AR}{E\beta} - \frac{E}{2.3RT} \tag{9}$$

Accordingly log $[g(\alpha)/T^2]$ is to be calculated for all possible mechanisms and the best straight line determines the operating mechanism. E and A can be calculated from the slope and the intercept.

One of the difficulties encountered when using this technique is that more than one mechanism fit the results [7]. To explain this observation reference should be made to Table 1.

It is obvious that $\log g(\alpha)_{D_3} = 2 \log g(\alpha)_{R_3}$ + constant and $\log g(\alpha)_{A_3} = n \log g(\alpha)_{A_2}$. This indicates that both R_3 and D_3 will give straight lines with different slopes. Accordingly the activation energy for D_3 will be double the calculated value for R_3. Similarly if one of the Avrami–Erofeev mechanisms operate, A_2 and A_3 will give straight lines with different slopes. Moreover Criado and Morales [8] reported that D_2 and R_2 are related by the equation

$$\ln(1-\alpha)[\ln(1-\alpha)+\alpha] = 1.89 \ln\left[1-(1-\alpha)^{1/2}\right] + 0.4$$

and that D_4 and R_3 are related by the equation

$$\ln\left[(1-2\alpha/3)-(1-\alpha)^{2/3}\right] = 1.84 \ln\left[1-(1-\alpha)^{1/3}\right] - 0.46$$

The above equations indicate that differentiation between D_3, D_4 and R_3 or D_2 and R_2 is difficult and give relations between the various slopes (activation energy corresponding to various mechanisms). To differentiate between these mechanisms, Criado and Morales [8] recommended using isothermal techniques in addition to TG curves.

Another difficulty, which was also reported by various authors [7,9], is that the values $g(\alpha)$ for nucleation mechanisms are much smaller than others leading to straight line fits. This may lead to the wrong conclusion that these mechanisms are the controlling steps.

To overcome the above difficulties, Gadalla [7] used the values he obtained (following Kissinger's [11], Reich's [5] and Carroll and Manche's [2]

equations) for the average activation energies as a guide to differentiating between the best possible mechanisms.

Another way to overcome the tediousness of this trial and error approach is to integrate eqn. (6) and write the result in the form

$$g(\alpha) = [AE/R\beta]p(x) \tag{10}$$

where $p(x)$ is a function depending on both temperature and activation energy and has been tabulated by various authors. To facilitate calculations Šatava and Škvàra [10] plotted $p(x)$ vs. T for various activation energies and tabulated the values of $g(\alpha)$ for various mechanisms. They demonstrated that

$$\log g(\alpha) - \log p(x) = \text{constant} = \log(AE/R\beta) \tag{11}$$

Values of $\log g(\alpha)$ are plotted vs. T for all possible mechanisms and are put on the top of $\log p(x)$ chart so that the temperature scales coincide. The curves are then shifted along this ordinate until one of the $\log g(\alpha)$ curves fits one of the $\log p(x)$ curves. The activation energy can be read and the equation governing the kinetics established.

It should be mentioned that Kissinger [11] was one of the earlier workers who used DTA to calculate the activation energy. Based on the assumption that the peak temperature of DTA (T_p) is close to the temperature of maximum rate (T_m), Kissinger derived his equation assuming a power-law kinetic equation (eqn. 1).

$$\ln A = \ln(E/R) - \ln\left(T_p^2/\beta\right) + E/RT_p \tag{12}$$

Plotting $\ln(T_p^2/\beta)$ vs. $1/T_p$ will give a straight line of slope E/R. Ravindran et al. [12] proved that this equation gives accurate results only if T_p is close to T_m. Accordingly the present author used Kissinger's equation with T_m (read from DTG curves) instead of T_p.

It should be noted that difference differential methods are not popular because of the magnification of experimental scatter and accordingly they were not reviewed.

PREVIOUS WORK

Extensive work was carried out on the dissociation of calcium oxalate monohydrate and on calcination of $CaCO_3$. Table 2 summarizes the techniques used and the results obtained for the three established steps. It is clear that most research workers adopted equations for homogeneous reactions.

For the dehydration step $n = 2/3$ or unity. Excluding the result obtained by the difference differential method due to lack of accuracy as already explained, three-dimensional phase boundary movement can be assumed.

TABLE 2

Previous work on dissociation of calcium oxalate monohydrate

Reaction	Author(s)	Mechanism	Results		Method used
			E	$\ln A$	
$CaC_2O_4 \cdot H_2O = CaC_2O_4 + H_2O$	Coats and Refern [6]	$n = 0.71$	21.4		Equation (9) assuming power law, in air, Pt crucible
	Ninan and Nair [13]	$R_3(n = 0.65)$	$19.8 + 35.8/\beta$		Modified Coats and Redfern method, eqn. (9)
	Gurrieri et al. [14]		21	21.1	Kissinger's method, eqn. (12), air and N_2
	Maciejewski [15]		23		Two different heating rates
	Segal and Fatu [16]	$n = 1.1-1.2$	23–22		Difference differential assuming power law
	Tanaka et al. [17]	A_2			Isothermal and modified Coats and Redfern method, eqn. (9)
$CaC_2O_4 = CaCO_3 + CO$	Coats and Redfern [6]	$n = 0.38$	62		Power law, eqn. (9), in air
	Gurrieri et al. [14]		75	49	Kissinger's method, eqn. (12), air and N_2
$CO + 1/2\ O_2 = CO_2$	Ninan and Nair [13]	$R_2(n = 1/2)$			Modified Coats and Redfern method, eqn. (9)
$CaCO_3 = CaO + CO_2$	Coats and Redfern [6]	$R_2(n = 0.46)$	52		Power law, eqn. (9), air
	Sharp and Wentworth [1]	$n = 1/2$ or $2/3$	44–46		Power law, eqns. (9)+(5)
	Gurrieri et al. [14]		41	17.6	Kissinger's method, eqn. (13), air and N_2
	Criado and Morales [8]	R_3	40		Isothermal
		R_3, D_3, D_4	40, 80, 74		Modified Coats and Redfern method, eqn. (10)
		R_3	40		Isothermal, Coats and Redfern method

Recently, however, Tanaka et al. [17] demonstrated the difficulty in establishing the mechanism and proposed the Avrami–Erofeev mechanism, A_2.

For the dissociation of the anhydrous oxalate to $CaCO_3$, different mechanisms were suggested and it is astonishing that the kinetic parameters obtained in air and N_2 were identical [14] in spite of the fact that in air the evolved CO oxidizes to CO_2.

For the dissociation of $CaCO_3$ to CaO conflicting results were reported but it seems that combining isothermal results with the possibilities obtained with a constant heating rate [8] fixes the operating mechanism accurately as phase boundary movement with spherical symmetry.

Nothing has been reported on hydrated magnesium oxalate. Moodie et al. [18] used transmission electron micrographs to show that dissociation of $MgCO_3$ proceeds from nucleation sites on the surface of $MgCO_3$ platelets and proposed that the decomposition mechanism is phase boundary migration R_2 (two-dimensional movement with cylindrical symmetry).

EXPERIMENTAL AND RESULTS

Analytical grades of calcium oxalate monohydrate and magnesium oxalate dihydrate were heated in the Derivatograph in air using a platinum crucible. In each run, 500 mg were used and the reference material was calcined alumina. The combined thermal curves are shown in Figs. 1 and 2. Thermal curves for the calcium salt are in agreement with previous work.

Dissociation steps for hydrated magnesium oxalate

Dehydration begins at 190–220°C and ends at 280–340°C depending on the heating rate and from the weight changes, it is obvious that the endothermic reaction

$$MgC_2O_4 \cdot 2\,H_2O = MgC_2O_4 + 2\,H_2O$$

occurs. On further heating, it appears from the DTA curves that three reactions overlap in the temperature range 420–620°C. At the end of these reactions active magnesia is produced and the weight loss corresponds to the removal of one mole of CO and one mole of CO_2. With a heating rate of 13 K min^{-1} the exothermic effect is observed with the beginning of the loss and the tail consists of a pure endothermic peak implying that CO evolves first and oxidizes to CO_2 according to the reactions

$$MgC_2O_4 = MgCO_3 + CO \text{ (endothermic)}$$

$$CO + 1/2\,O_2 = CO_2 \text{ (exothermic)}$$

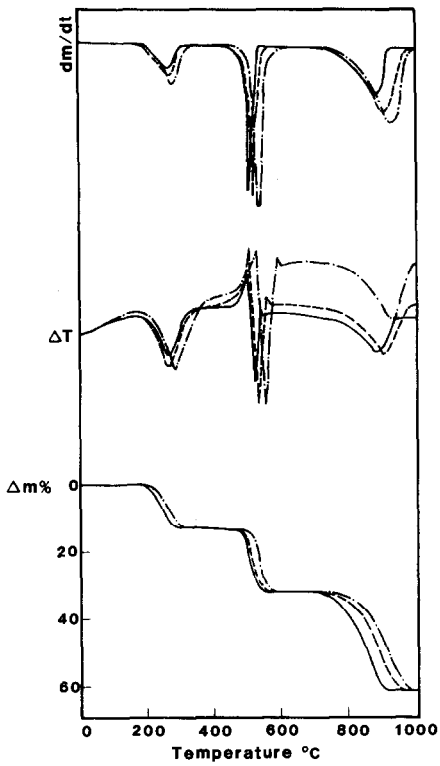

Fig. 1. Thermal curves for $CaC_2O_4 \cdot H_2O$. (————), 7 K min^{-1}; (- - - - -), 10 K min^{-1}; (· – · – ·), 12 K min^{-1}.

followed by dissociation of $MgCO_3$

$MgCO_3 = MgO + CO_2$ (endothermic)

With a lower heating rate of 6.7 K min^{-1}, the overlap of exothermic and endothermic peaks suggests that the three reactions occur simultaneously.

Dissociation mechanisms and kinetic parameters

As already explained, to obtain correct results using Kissinger's technique, DTG curves and not DTA were used and temperatures corresponding to maximum dissociation rates were used instead of peak temperatures on DTA. For each step, ln (T^2/α) was plotted against $1/T$ [eqn. (12)]: a typical straight line is shown in Fig. 3 for the dissociation of anhydrous magnesium oxalate. The slope of the straight line is E/R. The results obtained for the various dissociation steps for the two hydrates are indicated in Tables 3 and 4.

Reich's equation [eqn. (8)] was used to give the activation energy for each pair of heating rates. Average values for each step were calculated and are also indicated in Tables 3 and 4.

It should be noted that the methods described are based on the assump-

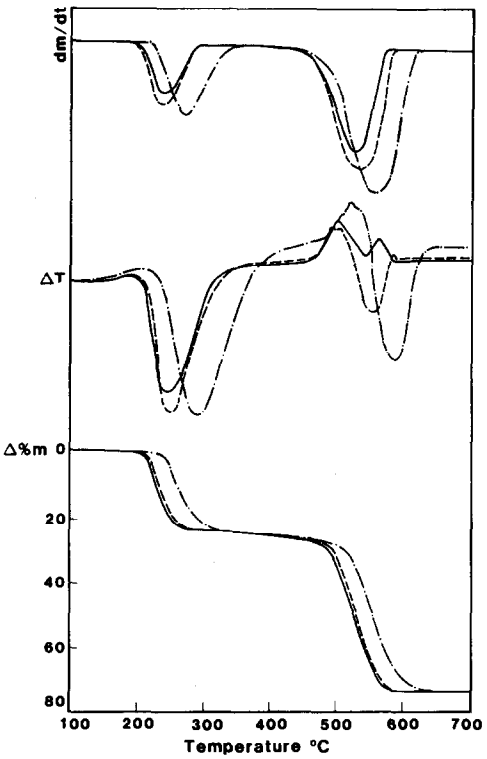

Fig. 2. Thermal curves for $MgC_2O_4 \cdot 2\ H_2O$. (————), 6.7 K min^{-1}; (- - - - -), 10 K min^{-1}; (· – · – ·), 13 K min^{-1}.

tion that the corresponding reactions proceed over narrow temperature ranges. Unfortunately, dissociation of MgC_2O_4 was found to exist over a temperature range wider than the range 0.9 T_m–1.1 T_m.

For each step, curves showing α vs. T were also constructed for the three heating rates using the equation $\alpha = (m_0 - m_t)/(m_0 - m_v)$. Fixed values of α were selected and the slopes of the best straight lines, obtained by plotting $\beta d\alpha/dT$ vs. $1/T$ on a semi-log paper, were used to calculate the activation energies using eqn. (5). Average values are shown in Tables 3 and 4 under the column headed "Carroll and Manche".

To determine the rate-determining mechanism for each step and the corresponding kinetic parameters, two techniques were used.

Coats and Redfern's equation

For each step, TG curves were used to calculate log $[g(\alpha)/T^2]$ for each possible controlling mechanism (Table 1) and were plotted against $1/T$. Such curves are shown in Fig. 4 for $CaCO_3$ when a heating rate of 7 K min^{-1} was used. According to eqn. (9) the best straight line fitting the points determines the mechanism and fixes E and A. One of the difficulties observed is that more than one straight line fits the results (Fig. 4). All

TABLE 3

Possible controlling processes and kinetic parameters for dissociation of calcium oxalate monohydrate in air with a heating rate of 7 K min^{-1}

	DTG			TG				
	Kissinger	Reich	Carroll and Manche	Coats and Redfern			Šatava and Škvàra	
	E	E_{av}	E_{av}	Mechanism	E	A	Mechanism	E
$CaC_2O_4 \cdot H_2O = CaC_2O_4 + H_2O$				A_2	14	1.4×10^5	A_2	15
				or A_3 [a]	9	5.5×10^2	or A_3 [a]	10
				or F_1	30	8.1×10^{11}	or F_1	30
				or R_1	24	1.0×10^9	or R_1	25
				or R_2	27	1.1×10^{10}	or R_2	30
				or R_3 [a]	28	3.0×10^{10}	or R_3 [a]	30
				or D_1	49	5.6×10^{19}		
				or D_2	53	1.6×10^{21}	or D_2	55
				or D_3	58	2.9×10^{22}	or D_3	60
	10	15	17	followed by			followed by	
				F_1	18	9.9×10^6	F_1	20
				or R_2	8	1.4×10^2	or R_2	20
				or R_3	11	1.4×10^3	or R_3	10
$CaC_2O_4 = CaCO_3 + CO$ $CO + 1/2\ O_2 = CO_2$	19	17	33	A_3	23	3.4×10^5	A_3	30
$CaCO_3 = CaCO + CO_2$				F_1	45 [b]	1.6×10^7		
	43	41	18	or R_3	54 [b]	4.2×10^8	R_3	47

[a] Best fits were obtained with A_3 and R_3. The latter was selected since it is known that nucleation mechanisms give lower values with misleading results (see above).

[b] R_3 was selected since Šatava & Škvàra's technique showed that the results fit only R_3.

TABLE 4

Possible controlling processes and kinetic parameters for dissociation of magnesium oxalate dihydrate in air with a heating rate of 13 K min^{-1}

	DTG			TG				
	Kissinger	Reich	Carroll and Manche	Coats and Redfern			Šatava and Škvàra	
	E	E_{av}	E_{av}	Mechanism	E	A	Mechanism	E
$MgC_2O_4 \cdot 2\ H_2O = MgC_2O_4 + 2\ H_2O$				A_2	22	5.1×10^8		
				or A_3	14	1.7×10^5	A_3	15
				or F_1	49	4.5×10^{19}	or F_1	50
				or R_1	44	3.0×10^{17}	or R_1	50
				or R_2	46	1.9×10^{18}		
				or R_3	47	2.2×10^{18}		
	12	12	7	followed by			followed by	
				A_2	9	1.3×10^3	A_2	10
				or A_3	5	1.8×10^1	or A_3	5
				or F_1	21	1.3×10^8	or F_1	20
				or R_2	10	1.3×10^3		
				or R_3	13	1.5×10^4	or R_3	15

$MgC_2O_4 = MgCO_3 + CO$ $CO + 1/2\ O_2 = CO_2$				A_2	28	6.5×10^6		
				or A_3	18	6.9×10^3	A_3 [a]	10 [a]
				or F_1	59	1.5×10^{15}	or F_1	45
				or R_1	53	2.9×10^{13}	or R_1	45
				or R_2	55	4.0×10^{13}		
				or R_3	56	8.1×10^{13}		
				or D_2	110	1.4×10^{28}		
				or D_3	117	3.9×10^{29}		
	25	25	25	followed by			followed by	
$MgCO_3 = MgO + CO_2$				A_2	15	1.1×10^3	A_2	10
				or A_3	8	1.4×10^1		
				or F_1	32	9.2×10^7	or F_1	30
				or R_2	15	4.4×10^2		
				or R_3	19	6.8×10^3	or R_3 [a]	25 [a]

[a] Using a heating rate of 10 K min^{-1} the activation energy increased to 20 and A increased to 2.6×10^4 for the first reaction but the activation energy and A for the second reaction did not change.

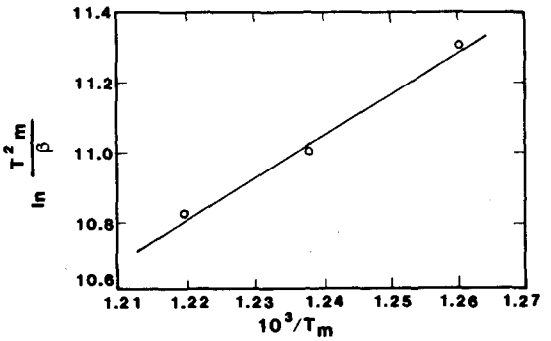

Fig. 3. Determination of the activation energy for the reaction $MgC_2O_4 + 1/2\ O_2 = MgO + 2\ CO_2$ using Kissinger's method.

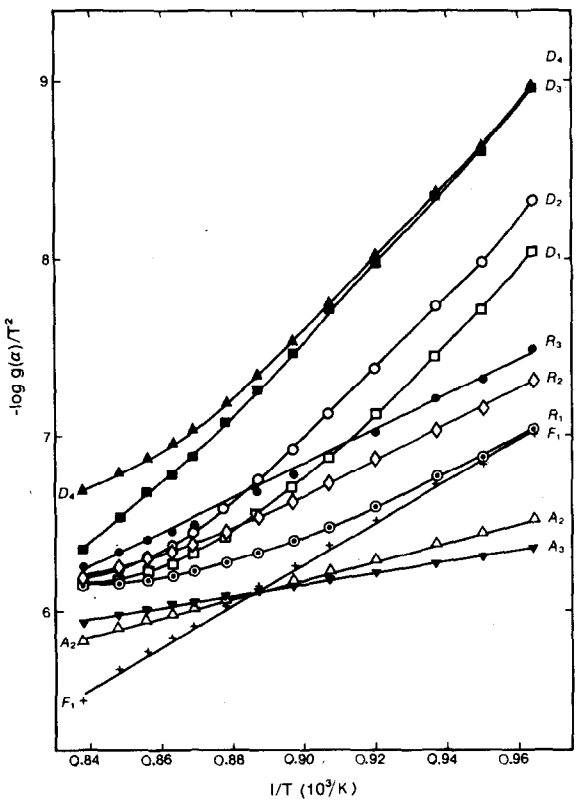

Fig. 4. Variation of $\log g(\alpha)/T^2$ with $1/T$ for dissociation of $CaCO_3$. Heating rate, 7 K min^{-1}.

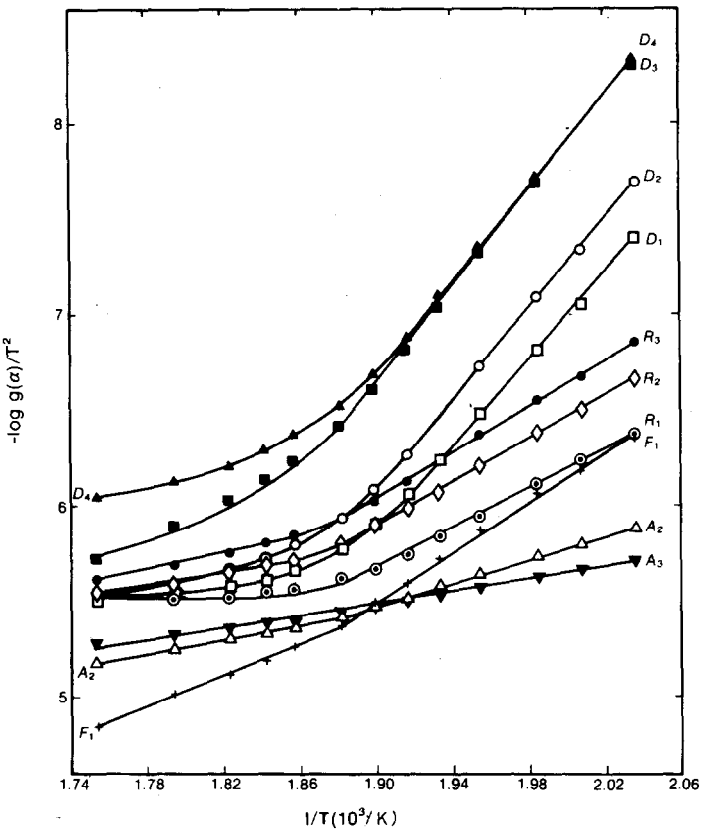

Fig. 5. Variation of log $g(\alpha)/T^2$ with $1/T$ for the dehydration of $CaC_2O_4 \cdot H_2O$. Heating rate, 7 K min^{-1}.

possible controlling mechanisms and the corresponding kinetic parameters are shown in Tables 3 and 4 under the columns headed "Coats and Redfern", separated by "or". For all steps other than those dealing with dissociation of anhydrous calcium oxalate and $CaCO_3$ it was difficult to find a straight line fitting all the experimental points. It was considered that more than one mechanism operates for each step and two straight lines were selected. Figure 5 was constructed for the dissociation of $CaC_2O_4 \cdot H_2O$ to CaC_2O_4 using a heating rate of 7 K min^{-1} and is shown to demonstrate this difficulty. The set of parameters which may operate at low temperatures were calculated and are indicated first, in Tables 3 and 4, followed by those corresponding to possible high-temperature mechanisms.

Šatava and Škvàra's technique

A chart showing the variation of log $p(x)$ with T was constructed and a set of curves were obtained for various activation energies. Values of log $g(\alpha)$ for the possible controlling mechanisms (Table 1) were calculated and plotted against T on a transparent paper using the same scales used for

constructing p(x). Figure 6 shows such curves obtained for $CaCO_3$ using a rate of 7 K min^{-1}. Šatava and Škvàra's technique, discussed earlier, was used and the values of activation energies read from the chart are shown in Tables 3 and 4.

If more than one g(α) curve coincides with the p(x) curves, all possible mechanisms are shown in the Tables separated by "or" and the corresponding activation energies are reported. Alternatively, if no curve for g(α) coincides completely with any p(x) curve, this indicates that more than one mechanism operates. Values obtained at lower temperatures are reported first, followed by those corresponding to the higher-temperature mechanism(s).

It was noted that when Coats and Redfern's technique or Šatava and Škvàra's technique was applied for the same reaction, the activation energy and the pre-exponential factor decreases with increasing heating rate. It should be noted that Ninan and Nair [13] published equations relating the change in the kinetic parameters as a function of the heating rate and the mass of the specimen.

The reason that the results over a limited temperature range fit more than one mechanism was explained above and values of activation energies obtained in the present work using Kissinger's, Reich's or Carroll and Manche's techniques were used to select the operating mechanisms underlined in Tables 3 and 4.

It is evident from Tables 3 and 4 that methods based on the maximum rate temperature could not differentiate between overlapping mechanisms or reactions and give only one value which was considered here to be an average value.

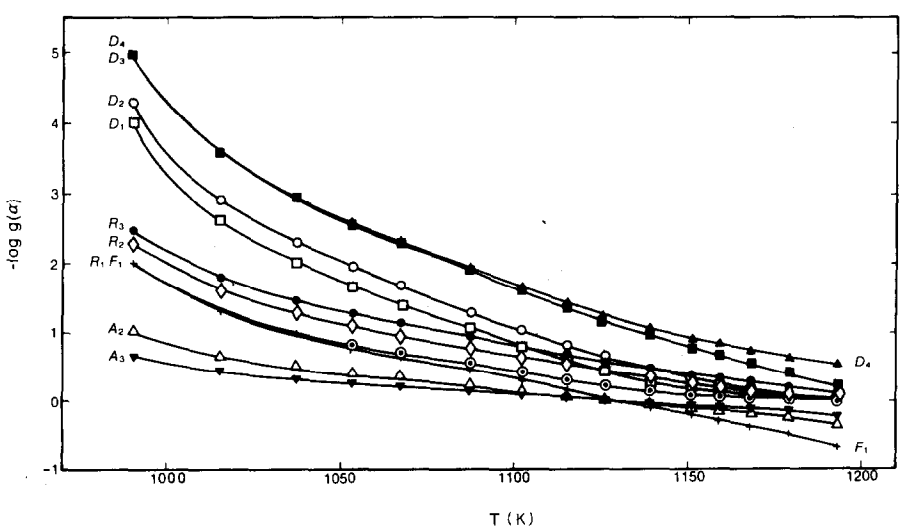

Fig. 6. Variation of log g(α) with temperature for the dissociation of $CaCO_3$. Heating rate, 7 K min^{-1}.

It is to be remembered that in all the methods investigated the activation energy and pre-exponential factors were considered constant. However, if we consider the results obtained for the dissociation of hydrated calcium and magnesium oxalates to the anhydrous oxalates it is evident that in each case the same mechanism operates but the values of E and A vary considerably. It could be concluded that these values vary regularly over the operating temperatures. This conclusion implies that the theoretical section of this paper will be only correct if the changes in these values are small and average values are used in the derived equations. Accordingly, Reich's [5] and Kissinger's [11] methods are not suitable for reactions occurring over wide temperature ranges or when activation energy and pre-exponential factors vary over wide ranges. Similarly, Carroll and Manche's [2] method assumes that the same mechanism operates over the range of temperatures at which the same values of α are reached with constant activation energy and pre-exponential factor. In view of the above results this may not be true. Moreover, the results are very sensitive to slight variations in the slope $d\alpha/dT$ and are not reliable but these values are just sufficient to select the operating mechanism using Coats and Redfern's technique or Šatava and Škvàra's technique.

The number of possible mechanisms obtained using Šatava and Škvàra's technique is much less than the number obtained by Coats and Redfern's technique and accordingly the latter technique is recommended. Only in cases when the possible mechanisms have close activation energies or very low activation energies the two techniques should be followed to select the best fit.

CONCLUSIONS

Dehydration of hydrated calcium and magnesium oxalates demonstrate that for the same reaction and the same mechanism the activation energy and pre-exponential factor can vary over wide ranges. Accordingly, methods based on expressing the maximum rate temperature as a function of heating rate, such as Kissinger's and Reich's methods, are not suitable for such cases.

Carroll and Manche's technique was found to be very sensitive to slight variations in the slope $d\alpha/dT$ and is not reliable. In addition to this, they assume that the same mechanism operates, with the same kinetic parameters, over the range of temperatures at which the same percentage decomposition is reached.

The above methods could not differentiate between overlapping mechanisms or reactions. Methods based on the modified equation of Coats and Redfern or on Šatava and Škvàra's technique can differentiate between the operating mechanism, can overcome the changes in kinetic parameters with temperature and can fix them more accurately. The disadvantage of these

techniques is that more than one possible mechanism with completely different kinetic parameters may be produced. Coats and Redfern's mechanism gave more possibilities and the reasons for this have been discussed. To overcome these difficulties it is recommended that the activation energy is approximately determined using Carroll and Manche's technique from various heating rates and this value is used to select the operating mechanism. When possible mechanisms have close activation energies both techniques (Coats and Redfern as well as Šatava and Škvàra) are needed to select the best fit.

Although dissociation of anhydrous magnesium oxalate and of $MgCO_3$ overlap, the initial part yields sufficient information that both Mg and Ca oxalates dissociate according to the Avrami–Erofeev nuclei growth mechanism A_3, whereas the tail end of the overlap was used to show that $MgCO_3$ dissociates in a manner similar to $CaCO_3$ according to phase boundary migration with spherical symmetry.

ACKNOWLEDGMENT

The author wishes to acknowledge the help of Dr. Ahmed Nasr-El-Din for running the Derivatograph used to obtain the thermal curves.

REFERENCES

1 J.H. Sharp and S.A. Wentworth, Anal. Chem., 41 (1969) 2060.
2 B. Carroll and E.P. Manche, Thermochim. Acta, 3 (1972) 449.
3 D.W. Van Krevelen, C. Van Heerden and F.J. Huntjens, Fuel, 30 (1951) 253.
4 H.H. Horowitz and G. Metzger, Anal. Chem., 35 (1963) 1464.
5 L. Reich, J. Polym. Sci., 2 (1964) 621.
6 A.W. Coats and J.P. Redfern, Nature (London), 201 (1964) 68.
7 A.M. Gadalla, Int. J. Chem. Kinet., accepted for publication.
8 J.M. Criado and J. Morales, Thermochim. Acta, 19 (1977) 305.
9 M.C. Ball and M.J. Casson, Thermochim. Acta, 27 (1978) 387.
10 V. Šatava and F. Škvàra, J. Am. Ceram. Soc., 52 (1969) 591.
11 H.E. Kissinger, J. Res. Natl. Bur. Stand., 57 (1956) 712.
12 P.V. Ravindran, T.P. Radhakrishnan and A.K. Sundaram, Bhabba Atomic Research Center, Bombay, India, BARC, Rep. 927, 1977, 47 pp.
13 K.N. Ninan and C.G.R. Nair, Thermochim. Acta, 37 (1980) 161.
14 S. Gurrieri, G. Siracusa and R. Cali, J. Therm. Anal., 6 (1974) 293.
15 M. Maciejewski, Rocz. Chem., Ann. Soc. Chim. Polonorum, 51 (1977) 535.
16 E. Segal and D. Fatu, J. Therm. Anal., 9 (1976) 65.
17 H. Tanaka, S. Ohshime, S. Ichiba and H. Negita, Thermochim. Acta, 48 (1981) 137.
18 A.F. Moodie, C.E. Warble and L.S. Williams, J. Am. Ceram. Soc., 49 (1966) 676.
19 J. Zsakó, J. Phys. Chem., 72 (1968) 2406.